Water Research X 17 (2022) 100162

Contents lists available at ScienceDirect

Water Research X

journal homepage: www.sciencedirect.com/journal/water-research-x

Amyloid adhesin production in activated sludge is enhanced in lab-scale sequencing batch reactors: Feeding regime impacts microbial community and amyloid distribution

An-Sofie Christiaens, Manon Van Steenkiste, Koen Rummens, Ilse Smets *

KU Leuven, Chemical Engineering Department, Chemical and Biochemical Reactor Engineering and Safety (CREaS), Celestijnenlaan 200f box 2424, Heverlee 3001, Belgium

ARTICLE INFO

Keywords:
Biological wastewater treatment
Bioflocculation
Extracellular polymeric substances
Thioflavin T
CLSM
Microbial community

ABSTRACT

Amyloid adhesins are β-sheet-rich extracellular proteins thought to contribute to bioflocculation. They are present in activated sludge to varying extent. However, it remains unclear which operational conditions promote their production. To this end, the abundance and distribution of amyloids and their potential producers were monitored in two lab-scale reactors operated in sequencing batch mode with an unaerated and aerated reaction phase. Various feeding regimes ranging from feast-famine to nearly continuous feeding were applied. Thioflavin T staining revealed more amyloids in the lab-scale reactors during all operational stages compared to the full-scale industrial and municipal inocula. Furthermore, the feeding regime impacted the distribution of produced amyloids from dense clusters during feast-famine conditions towards a dispersed distribution during nearly continuous feeding. This dispersed presence did not negatively impact the bioflocculation (towards average floc size and shear sensitivity). 16S rRNA sequencing detected several known EPS and amyloid producers. More continuous and, hence, partially aerobic feeding promoted the relative abundance of denitrifiers. Sequential Thioflavin T staining and fluorescence *in situ* hybridization identified *Zoogloea* and *Ca.* Competibacter as potential amyloid producers under the applied conditions. This experiment confirms that amyloid producers need to be triggered for production and that the feeding regime impacts the microbial community composition, which in turn influences the amyloid production and distribution.

1. Introduction

The performance and cost-efficiency of biological wastewater treatment systems highly depend on the ability of the activated sludge bacteria to form large and dense flocs such that an efficient sludge-water separation can be ensured. A crucial element for the structural integrity of these flocs is the matrix of extracellular polymeric substances (EPS) in which the activated sludge bacteria are embedded (Suresh et al., 2018). In the proteinaceous fraction of the EPS, various adhesins exist that are distinguished by their structure and specific mechanism of cell-to-cell interaction: e.g., flagella, pili, lectins, and amyloid adhesins. These latter structures are β-sheet-rich and highly organized proteins that are insoluble and resistant to many chemical and mechanical denaturants and protease activity (Christensen et al., 2020; Epstein and Chapman, 2008). Most of the information about the role of bacterial amyloids in bio-aggregation is inferred from pure culture biofilm studies of bacteria that have limited relevance in wastewater treatment, e.g., *E. coli, Pseudomonas*, and *Bacillus subtillis* (Aqeel et al., 2019). Amyloids improve the adherence properties and mechanical robustness of these biofilms. Inspired by these results from the domain of pure cultures, amyloid adhesins are thought to contribute to the high stability of the strongly bound fraction of cells and EPS in activated sludge flocs (Larsen et al., 2008) yet this hypothesis has not been investigated thoroughly to the best of the authors' knowledge. Nonetheless, amyloids have been detected in activated sludge systems in biofilms, flocs, and aerobic granules (Dueholm and Nielsen, 2016; Lin et al., 2018; Aqeel et al., 2021).

Pure culture studies on model organisms have revealed some conditions in which amyloid production is enhanced, such as low temperature, low oxygen content, low osmolarity, and nutrient limitation (e.g., Fe^{3+} limitation for *Pseudomonas*) (Gerstel and Römling, 2001; Maurer et al., 1998; Prigent-Combaret et al., 2001; Scharfman et al., 1996).

* Corresponding author.
E-mail address: ilse.smets@kuleuven.be (I. Smets).

https://doi.org/10.1016/j.wroa.2022.100162

Available online 28 November 2022

However, these observations are often organism dependent, or the applied conditions may not be possible or may be less appropriate to implement within the context of wastewater treatment. If amyloid adhesins can be linked to strong bioflocculation and if their production can be promoted by certain operational conditions, we have a powerful tool to optimize the sludge-water separation part of activated sludge systems. This work, therefore, (*i*) investigated the possibility of stimulating amyloid adhesin production in an activated sludge community by changing the feeding pattern in a sequencing batch reactor (SBR) setup, while (*ii*) screening the activated sludge bacterial community for the corresponding amyloid producers. The original research hypothesis was that a more continuous feeding would induce a decrease in adhesin production and a concomitant deterioration of the bioflocculation. The latter is monitored through floc size and strength.

2. Materials and methods

2.1. Parallel sequencing batch reactor set-up and operation

The reactors consisted of 4 L glass cylindrical vessels stirred using a magnetic stirring plate (Velp Scientifica). The reactor temperature was kept at 23 °C using an internal heating coil and a VWR™ water bath. Oxygen was supplied near the bottom of the reactor via a diffuser attached to an air pump (HS Aqua) providing 150 L air h^{-1}. Peristaltic pumps controlled the addition of synthetic wastewater and water and the removal of effluent, resulting in a constant hydraulic retention time of 48 h. A solid retention time of 20 days was achieved by manual daily wasting of the mixed liquor. A Velleman VM8090 8-channel USB relay card and Serial Port Tool Relay Timer R8X software controlled the equipment. A schematic of the used lab-scale sequencing batch reactor (SBR) setup is included in Fig. 1. The 6 h reaction cycle consisted of an anoxic (2 h) and aerobic phase (3.5 h), followed by sedimentation (20 min) and effluent withdrawal (5 min). Effluent was withdrawn from the top. The duration and frequency of the feeding were changed three times during the experiment, resulting in three different experimental stages as represented schematically in Fig. 2. In the first experimental stage, bioflocculation-inducing feast-famine conditions were applied by feeding once every cycle. In later stages, the carbon (C) and nitrogen (N) feeding 'stress' was relaxed: intermediate (every 72 min) or nearly continuous feeding (every 20 min) was applied.

The inoculum of the first reactor was obtained from a full-scale aerobic SBR treating wastewater from a food processing company on September 9, 2020. The inoculum of the second reactor was obtained from a full-scale aerobic municipal wastewater treatment plant operated by Aquafin (Leuven, Belgium) on September 2, 2020. The inocula were stored at 4 °C before use and diluted to 4.5 g MLSS L^{-1} with autoclaved tap water upon inoculation. The reactors were fed 0.174 g COD (g MLSS) $^{-1}$ d^{-1} with synthetic municipal wastewater with a composition of 85:6:1 C:N:P and a ratio of monovalent to polyvalent cations of 0.81. The wastewater was adapted from Van den Broeck et al. (2010) and consisted of 801 mg L^{-1} (CH3COO)2Ca.H2O, 895 mg L^{-1} $C_6H_{12}O_6$, 95.3 mg L^{-1} yeast extract, 335 mg L^{-1} NH_4Cl, 78.5 mg L^{-1} $(NH_4)_2HPO_4$, 45.0 mg L^{-1} KCl, 69.6 mg L^{-1} Na_2SO_4, 188 mg L^{-1} $MgCl_2{\cdot}6H_2O$, 57.5 mg L^{-1} $CaCl_2{\cdot}2H_2O$, and 9.11 mg L^{-1} $FeCl_3$.

2.2. Sludge characterization: amyloid detection and bioflocculation performance

Different approaches exist to fluorescently detect amyloids. The benzothiazole dye Thioflavin T (ThT) has long been the "gold standard" to detect protein misfolding in the medical field and has also been used to detect functional amyloids in bacteria. This dye is characterized by a large increase in fluorescence upon binding to amyloids (Biancalana and Koide, 2010). More recently, antibodies have also been used for amyloid detection: e.g., conformational antibodies WO1 and WO2 and antibodies against CsgA and CsgB curli proteins expressed in *E. coli* (Brei, 2011; Chapman et al., 2002; O'Nuallain and Wetzel, 2002). In this work, the Thioflavin T (ThT) dye was used to detect amyloid adhesins in the activated sludge sample as it is commercially available, unlike the mentioned conformational antibodies, and will bind to diverse amyloid structures in various organisms, unlike the sequence-specific antibodies.

ThT powder (Thermo Fisher Scientific) was dissolved in Milli-Q® water and filtered through a 0.2 μm syringe filter. The concentration of the stock solution was determined spectrophotometrically by absorbance measurement at 412 nm. From this, the concentration was calculated via the Lambert-Beer law with the molar extinction coefficient equal to 36 000 M^{-1} cm^{-1} for Thioflavin T in water (De Ferrari et al., 2001). To perform the staining, fresh samples were diluted to 1 g MLSS L^{-1}, ThT was added to a final concentration of 3 μM and incubated (15 min, room temperature).

The ThT fluorescence signal was visualized using an Olympus FluoView™ FV1000 confocal microscope equipped with 440 nm laser, 405–458 nm dichroic mirror, and 480–495 nm barrier filter. Laser intensity percentage and detector voltage were chosen such that all observable autofluorescence on an unstained sample was minimized. The transmission signal was collected as a reference. Image processing was performed in FIJI (Schindelin et al., 2012). The color intensity of the images was slightly adjusted for improved resolution.

The ThT fluorescence signal was quantified in a 96 well plate (art. no. 655090, Greiner bio one international GmbH, Kremsmünster, Austria) in four technical replicates using a Tecan infinite M200 pro microplate reader with i-control™ 1.9 software. An emission scan was performed

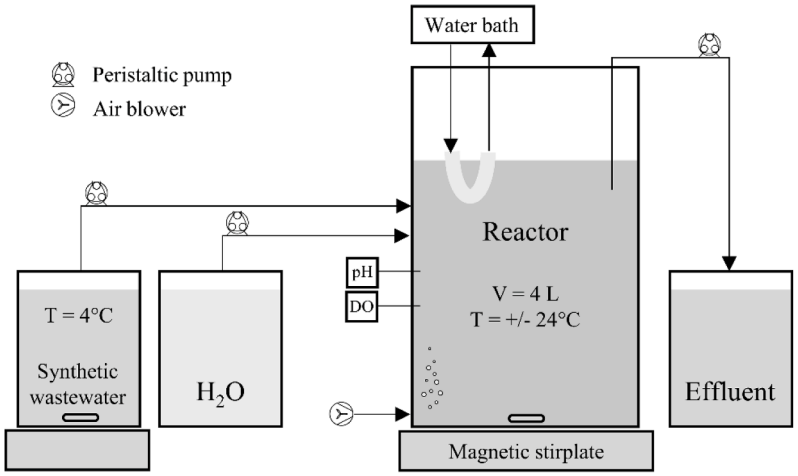

Fig. 1. Schematic representation of the reactor set-up.

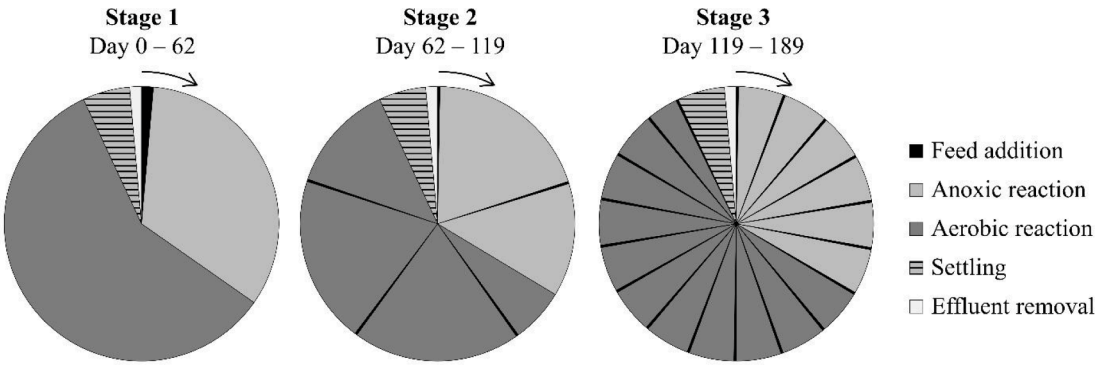

Fig. 2. Schematic representation of the operational cycles of the industrial and municipal lab-scale sequencing batch reactor set-up. Total cycle time: 6 h.

from 440 to 650 nm with a 10 nm stepsize and an excitation wavelength of 400 nm to minimize excitation light carryover. Quadruplicates of unstained samples and ThT in phosphate buffered saline (PBS) blank samples were included in all experiments. Graphs were generated using MS Excel.

Sludge morphology was monitored weekly using an Olympus IX83 inverted microscope with cellSens Dimension software and an in-house developed MATLAB®-based image analysis software (Jenné et al., 2007). Floc shear sensitivity was determined biweekly using the standardized shear reactor test described by Mikkelsen and Keiding (2002) with slight modifications. Briefly, 700 mL of 3.5 g MLSS L^{-1} sludge was sheared for up to 300 min in a baffled reactor at a constant shear intensity ($G = 800\ s^{-1}$). The turbidity of the supernatant was measured every 30 min. The shear sensitivity constant k_{ss} was calculated as the difference in estimates for the dispersed mass at equilibrium $m_{d,\infty}$ and the initial dispersed mass $m_{d,0}$ relative to the MLSS content (Eq. (1)).

$$k_{ss} = \frac{m_{d,\infty} - m_{d,0}}{MLSS} \quad (1)$$

2.3. General physico-chemical analyses

The chemical oxygen demand (COD) and concentrations of ammonia (NH_4^+), nitrite (NO_2^-), and nitrate (NO_3^-) were monitored weekly using Hach testkits on samples filtered through 0.6 μm pore size filters (Macherey-Nagel MN GF-3). The dissolved oxygen (DO) concentration and pH were measured every 15 min with an IntelliCAL® LDO101 DO probe and PHC101 pH probe, and logged using a HACH HQ40D multimeter. The reactor biomass concentration (mixed liquor suspended solids (MLSS)) was analyzed according to Standard Methods (Greenberg et al., 1992). Graphs were generated using MS Excel.

2.4. Microbial community analysis

Fresh sludge was centrifuged (10 min, 4 °C, 5000 g) in a precooled centrifuge. Supernatant was decanted and the pellet was flash-frozen in liquid nitrogen and stored at −80 °C. Simultaneous DNA and RNA extraction was performed using the RNeasy® PowerSoil® Total RNA Kit (12866-25, QIAGEN®) and the RNeasy® PowerSoil® DNA elution Kit (12867-25, QIAGEN®) following the manufacturer's instructions. 16S rRNA genes were amplified according to the 16S Metagenomic sequencing library preparation guidelines described in document 15044223 Rev. B provided by Illumina and using the universal primers S-D-Arch-0519-a-S-15 (5′-CAG CMG CCG CGG TAA-3′) and S-D-Bact-0785-b-A-18 (5′-TAC NVG GGT HTC TAA TCC-3′) (Klindworth et al., 2013; Lemoine et al., 2019), targeting the V4 hypervariable region of the 16S rRNA gene of both Bacteria and Archaea (Lemoine et al., 2019). The amplified material was purified using AMPure XP beads (Beckman Coulter Genomics) following the manufacturer's instructions. Additional library preparation steps were performed at Genomics Core Leuven followed by sequencing on the Illumina MiSeq platform. Raw sequencing data were delivered in fastq format, processed with the Qiime 2™ analysis package version 2019.10 (Bolyen et al., 2019), and finally taxonomically classified according to the SILVA small subunit database version, release 132 (April 2018) (Quast et al., 2013). Graphs were generated using MS Excel.

2.5. Fluorescence in situ hybridization and identification of amyloid producers via a sequential procedure

Fluorescence *in situ* hybridization (FISH) was performed as described by Amann (1995) using the probes described below. For direct identification of amyloid producers, an optimized protocol of sequential ThT staining and FISH is proposed, based on Larsen et al. (2007): first, activated sludge was stained with ThT, followed by an initial localization and recording of several flocs on a glass coverslip. After that, the sample was dried on the coverslip and, if still needed, fixed for 2 h with 4% paraformaldehyde (PFA) for fixation of Gram-negative cells. The dehydration and hybridization were performed as described by Amann (1995). Finally, the same flocs were localized again and recorded. To avoid biomass wash-off during this procedure, glass cover slips were pretreated by rinsing with 70% ethanol for degreasing, followed by dipping into 0.5% w/v gelatin and 0.01% $CrK(SO_4)_2$ at 70 °C to improve adhesion (Nielsen et al., 2009). To facilitate floc localization, coverslips with a 500 μm grid (Ibidi) were used.

The identity of some bacteria in sludge samples was investigated using the following oligonucleotide probes: ZRA23a targeting members of the *Zoogloea* lineage except *Z. resiniphila* (Rosselló-Mora et al., 1995), GAOmix (equimolar mixture of GB_G1 and GB_G2) for several *Ca.* Competibacter (Crocetti et al., 2002; Kong et al., 2002), and EUBmix (equimolar mixture of EUB-338, EUB338-II#, and EUB338-III) targeting most Bacteria (Amann et al., 1990; Daims et al., 1999). Details are summarized in probeBase (Loy et al., 2007). Probes were double-labeled at the 5′- and 3′-end with the same fluorophore: either 6-carboxyfluorescein (6-Fam) or the sulfoindocyanine dye Cy3. All probes were purchased from Biomers (Germany). The fluorescence signal was visualized on an Olympus FluoView™ FV1000 confocal microscope with a 488 nm laser and 505–540 nm barrier filter for 6-Fam and a 559 nm laser and 575–620 nm barrier filter for Cy3. Multi-channel datasets were recorded in sequential mode to avoid crosstalk.

3. Results

Results for the reactors inoculated with sludge from industrial and municipal origin are hereafter referred to as the industrial and municipal lab-scale SBR.

3.1. Evolution of amyloids detected with Thioflavin T

Samples subjected to different feeding conditions were characterized

using 3 μM ThT, targeting most amyloid adhesins. Visual detection based on microscopic images as well as quantification of the emission signal is performed.

As for the visual detection, Z-stack images were studied in 3-D, but are represented here in 2-D, as maximum intensity projections, with the transmission image included as a structural reference to distinguish unstained regions from voids (Fig. 3). In dense flocs, such as present in the industrial SBR at the end of the first operational stage, the light penetration was limited to a depth of around 25 μm, which should be considered when interpreting the CLSM results. ThT positive areas were abundant in the inoculum originating from the industrial wastewater treatment plant (WWTP) and detected as characteristic spherical clusters with a diameter of 11.16 +/− 4.19 μm ($N = 6$). In comparison, ThT positive areas were scattered and less abundant in the inoculum originating from the municipal plant. A qualitative increase in ThT positive areas was observed in both reactors during the first operational stage. In later stages, characterized by more frequent feeding, the ThT signal appeared less clustered and more evenly spread throughout the sludge floc. ThT also stained elongated structures representing filamentous bacteria or epiphytic attachments. The spatial arrangement of the fluorescent signal in the floc was further studied from the 3-D-reconstructions in "depth coding" mode with the "16 colors" color scale (Fig. 4): single optical sections are overlapped after attributing one color to each of them. Colors range from white to black corresponding to the lowest slice (i.e., closest to the objective) and highest slice (i.e., furthest away from the objective), respectively. This representation preserves some depth information in a 2-D image. The emission signal mostly appears to be present throughout the entire floc depth.

Additionally, the ThT emission signal of sludge suspensions was quantified at the excitation maximum of 490 nm. Results are corrected for sample autofluorescence and reported in Fig. 5. A similar trend was observed for both reactors. After inoculation, the fluorescence intensity steadily increased until an equilibrium was achieved at the end of Stage 1. After a delay, the signal then increased further in the later stages characterized by more frequent and, hence, aerobic feeding.

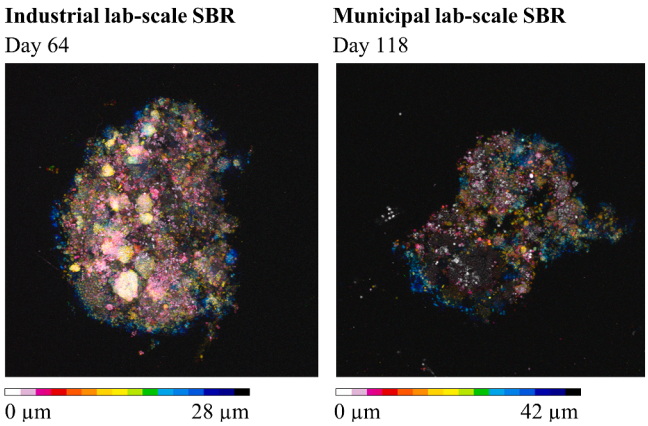

Fig. 4. 3-D "depth coded" reconstruction of the CLSM images assembled from the z-stack of optical sections with white to black "16 colors" color scale. Industrial and municipal lab-scale sequencing batch reactor (SBR) samples stained with 3 μM Thioflavin T.

3.2. *Bioflocculation performance*

The largest average floc size was observed in the industrial lab-scale reactor while subjected to feast-famine conditions (Fig. 6). Afterwards, the average floc size decreased gradually, and remained stable during the third operational stage. No strong trends were observed in the municipal lab-scale SBR, but the average floc size was generally the lowest when subjected to nearly continuous feeding (Stage 3).

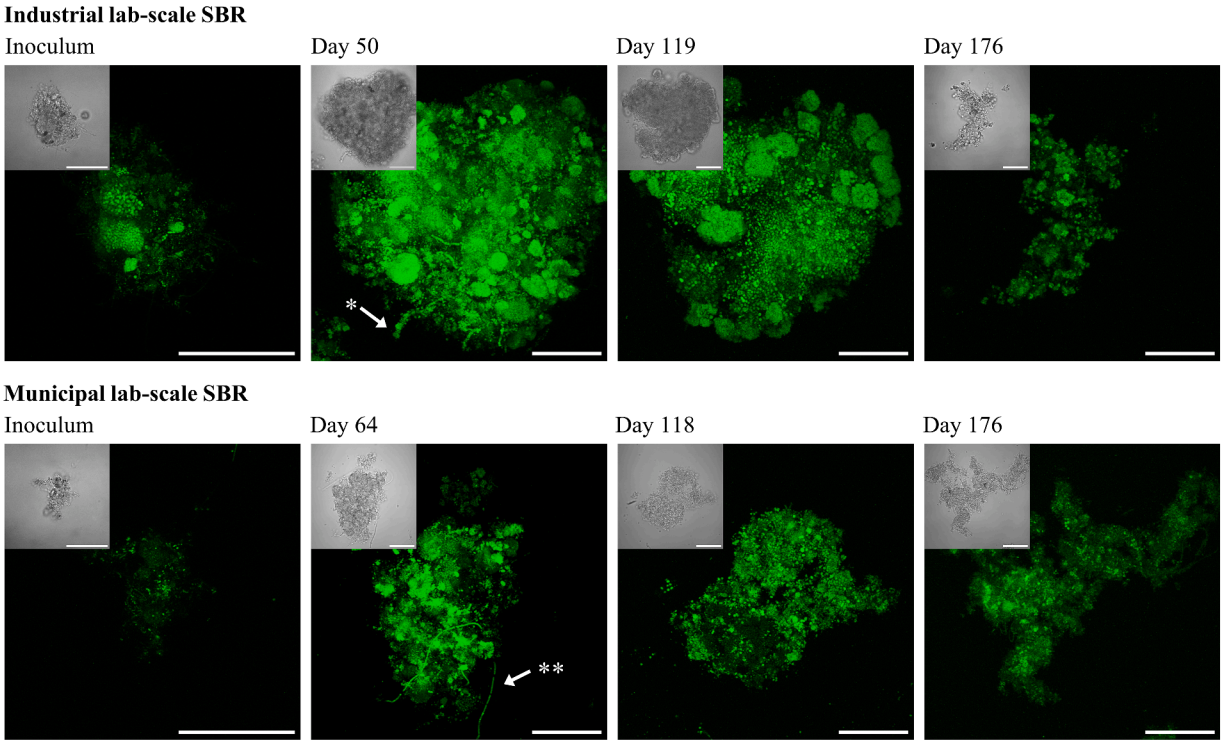

Fig. 3. Representative fluorescence CLSM and transmission images illustrating the morphology and location of amyloid adhesins in sludge flocs in the industrial and municipal lab-scale sequencing batch reactors (SBR). Samples stained with 3 μM Thioflavin T (ThT). Results shown for inoculum and the end of Stage 1 (day 50), the beginning (day 64) and end of Stage 2 (day 118), and the end of Stage 3 (day 176) where sludge was subjected to feeding once every 6 h, 72 min, and 20 min, respectively. Z-stacks are represented as maximum intensity projections. Arrows indicate a filament with ThT-positive epiphytic growth (*) and a ThT-positive filament (**). Scale bar = 50 μm.

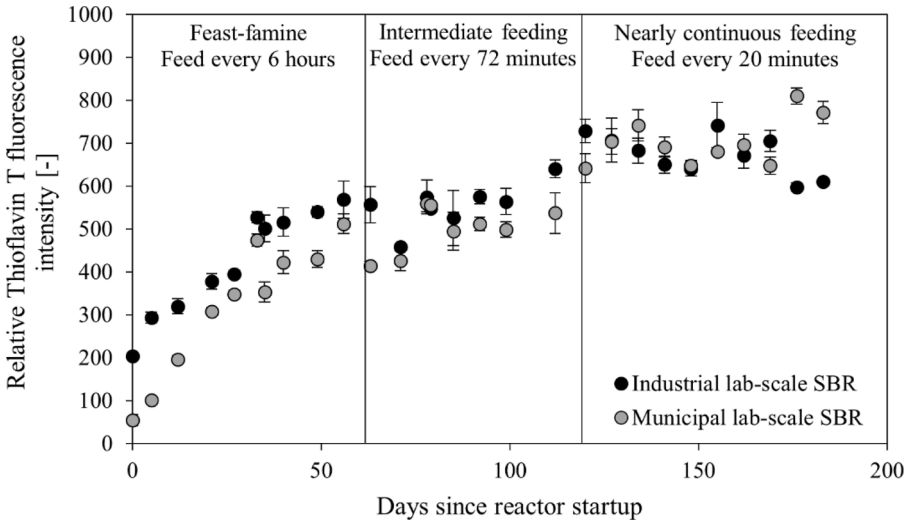

Fig. 5. Evolution of Thioflavin T fluorescence intensity (as an estimate of the amount of amyloids) at 490 nm in the industrial and municipal lab-scale sequencing batch reactors (SBRs). Sample stained with 3 μM Thioflavin T relative to unstained sample. Each value represents the average of four technical replicates. Error bars represent standard deviations.

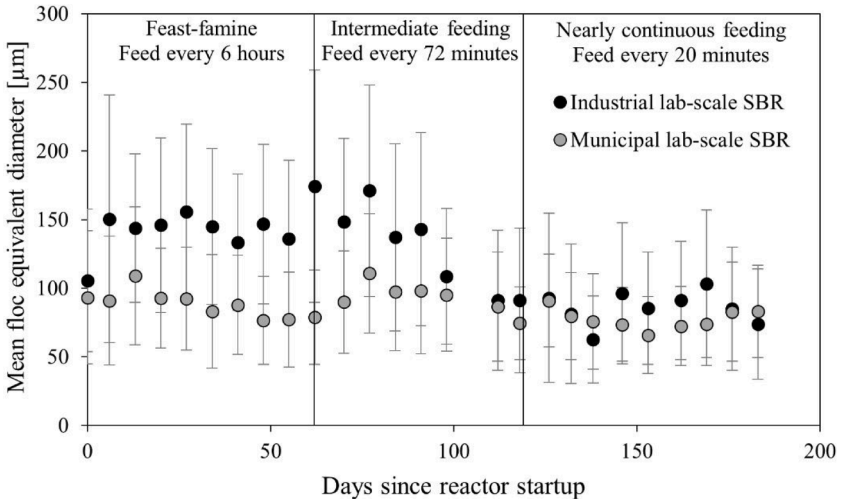

Fig. 6. Evolution of floc size represented as mean floc equivalent diameter, weighted with floc area, in the industrial and municipal lab-scale sequencing batch reactors (SBRs). Error bars represent standard deviations.

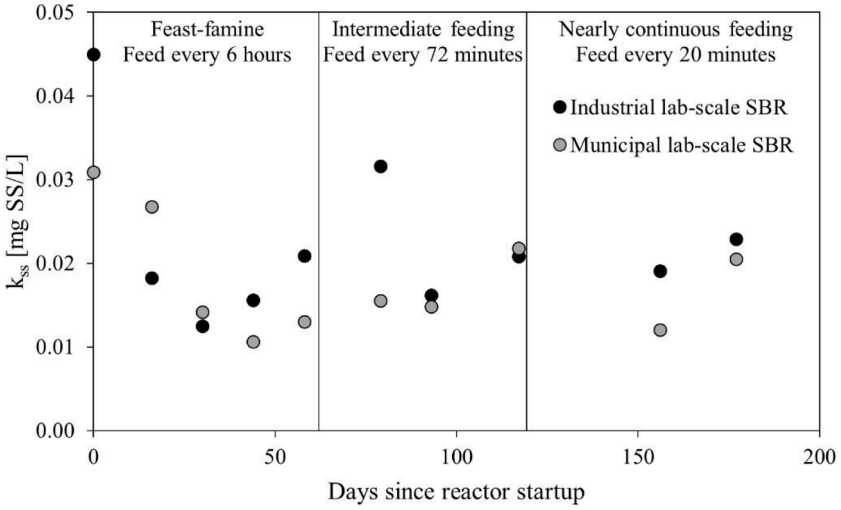

Fig. 7. Evolution of sludge shear sensitivity k_{ss} in the industrial and municipal sequencing batch reactors (SBRs).

Sensitivity to turbulent shear was relatively low for both reactors throughout the experiment with fluctuating values (Fig. 7). The lowest values for k_{ss} were measured near the end of the first operational stage (day 30 and 44 for industrial and municipal lab-scale reactor, respectively).

3.3. Reactor performance and community dynamics

The activated sludge community dynamics is first described on the family level to then zoom in on the genus level, which is finally correlated to the reactor performance.

By including an anoxic phase, the SBRs were expected to have a high nitrogen removal on top of the conventional organic carbon (COD) removal. Under aerobic conditions, autotrophic nitrifiers can oxidize NH_4^+ to NO_3^-, which, under anoxic conditions, heterotrophic denitrifiers can reduce to N_2. However, while a COD removal of at least 98.1% (industrial SBR) and 95.8% (municipal SBR) was achieved, the nitrogen removal was impaired after Stage 1, as discussed below.

On average 65 716.58 reads per sample ($N = 12$ samples) were obtained from Illumina MiSeq. Reads with a frequency lower than 18 were removed. This cut-off equals 0.05 percent of the average read abundance after DADA2 denoising.

At the family level (top part of Fig. 8), *Rhodocyclaceae* were detected in all stages but became more abundant in the industrial lab-scale SBR during Stages 2 and 3 of reactor operation with a 35.46% and 26.53% relative read abundance, respectively. At these time points also the *Flavobacteriaceae* were abundant with 21.58% and 8.58% in the industrial lab-scale SBR. In the municipal lab-scale SBR, the family *Competibacter* became more abundant in Stage 3.

At the genus level (bottom part of Fig. 8), the results are summarized here in functional groups. The abundance of ammonium and nitrite-oxidizing genera decreased for both reactors throughout the reactor run. These microbial community dynamics were reflected in an increase of NH_4^+ and a decrease of NO_3^- in Stage 3 (Fig. 10).

Regarding denitrifying bacteria, during Stage 1, *Rhodocyclaceae*-related *Zoogloea* were abundant in the industrial lab-scale SBR (increase to 10.74%), and in the municipal lab-scale SBR (maximum of 5.78%) (see also Fig. 9). The abundance of *Rhodocyclaceae*-related *Thauera* increased to 4.80% and 3.31% for the industrial and municipal lab-scale SBR, respectively. In the municipal lab-scale reactor, the abundance of *Dechloromonas* remained high with a maximum of 5.05%, and *Flavobacterium* was detected with an increased abundance with a maximum of 4.27%. However, the altered conditions in later operational stages including aerobic feeding and lower abundance of nitrifying bacteria also affected the denitrifying genera. In the industrial lab-scale reactor, *Flavobacterium* and *Zoogloea* became very abundant at Stage 2 (21.58%)

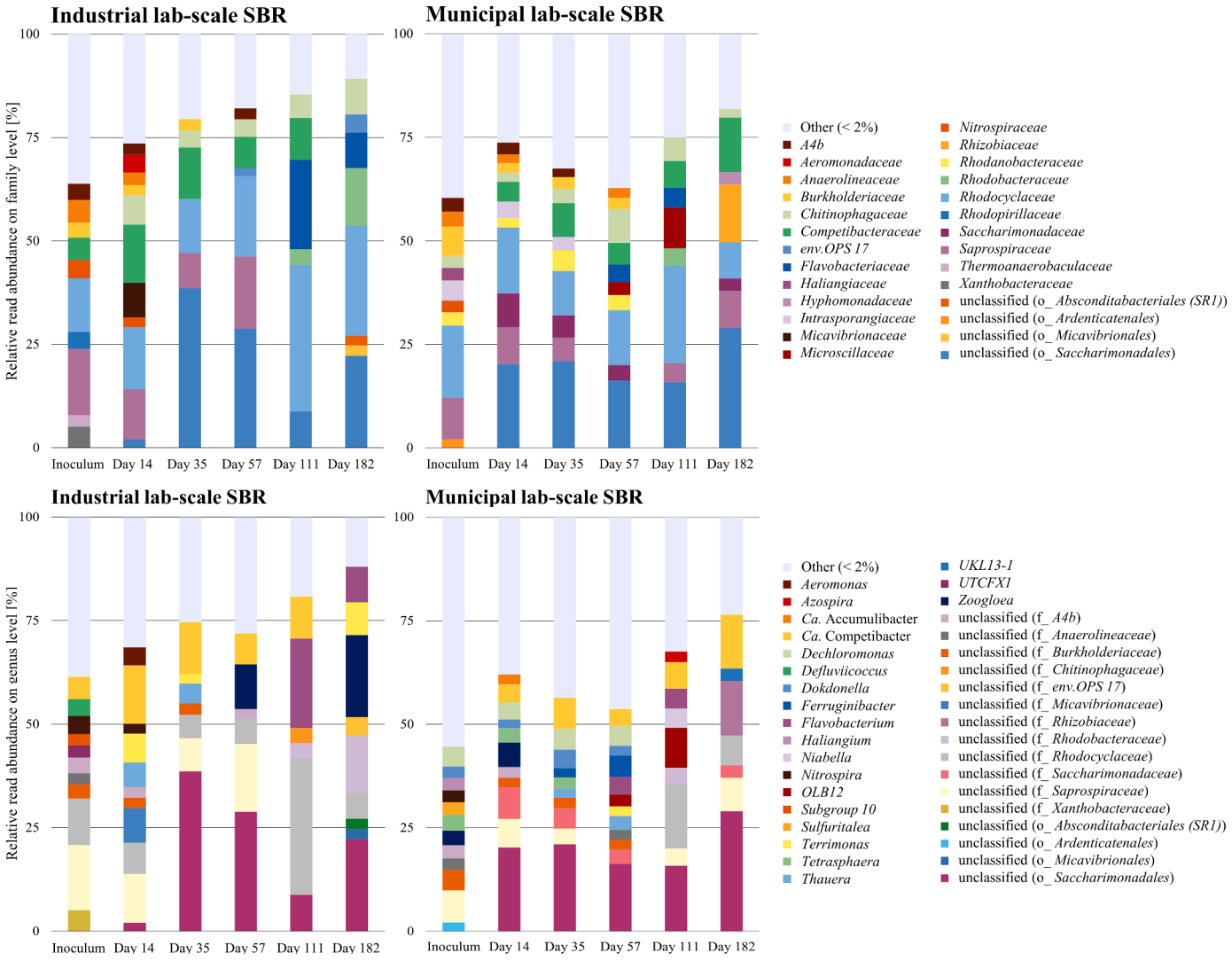

Fig. 8. Evolution of bacterial community composition in the industrial and municipal lab-scale sequencing batch reactors (SBR) on family (top) and genus (bottom) level. Families or genera with a relative read abundance lower than 2% were grouped in "Other (< 2%)". o_ = order, f_- = family.

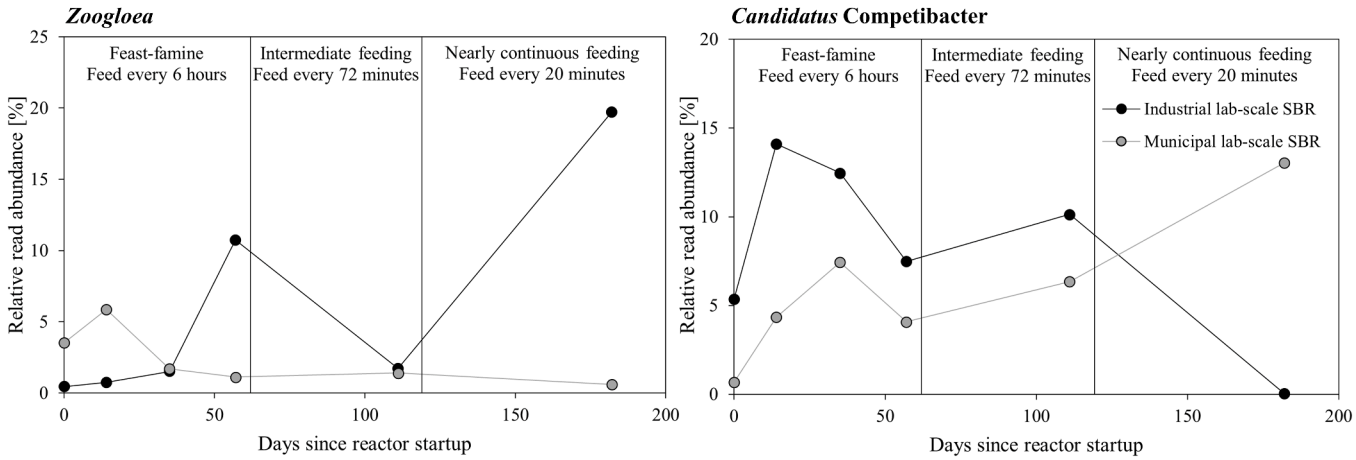

Fig. 9. Relative read abundance of *Zoogloea* and *Candidatus* Competibacter in the industrial and municipal lab-scale sequencing batch reactors (SBRs).

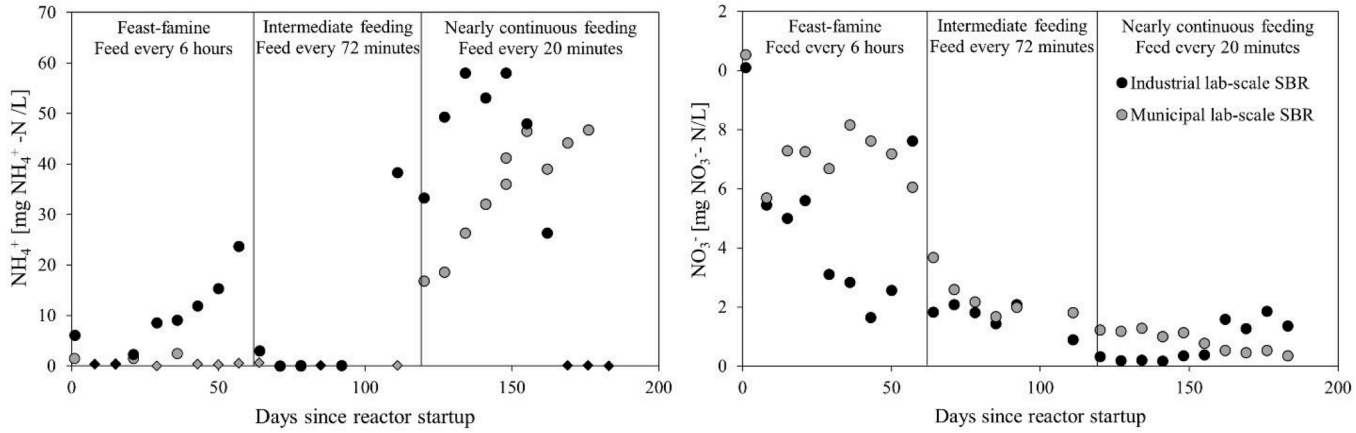

Fig. 10. Ammonium and nitrate in the industrial and municipal lab-scale sequencing batch reactors. Diamonds indicate values under the measuring range of the testkit. Samples were taken 5 min before the end of the aerobic reaction phase.

and Stage 3 (19.73%), respectively.

In both reactors, the abundance of almost all polyphosphate accumulating organisms (PAOs), e.g., *Actinobacterial* PAO *Tetrasphaera* and *Rhodocylus*-related PAO *Dechloromonas,* decreased during operational Stage 1. Only *Rhodocyclus*-related *Candidatus* Accumulibacter was detected in all stages with a maximum abundance of 2.39% in the municipal lab-scale SBR.

With respect to glycogen accumulating organisms (GAOs), the inocula contained mainly *Defluviicoccus* (4.07%, industrial), *Propionivibrio* (1.07%, municipal), and *Candidatus* Competibacter (5.35%, industrial) (see also Fig. 9). The abundance of the latter remained high in the industrial lab-scale reactor except in Stage 3. On the other hand, in the municipal lab-scale SBR, its abundance reached its maximum (13.02%) in this last stage.

3.4. Distribution of selected potential amyloid producers and comparison with Thioflavin T staining

The identity of amyloid adhesins producers was investigated using FISH (Fig. 11). Targets were selected based on their high abundance in our system, their correlation with a high total relative Thioflavin T (ThT) fluorescence intensity and their known EPS or amyloid producing capacities. Although the used probes are not completely genus-specific, the targeted bacteria will hereafter be referred to as *Zoogloea* (probe ZRA23a) and *Candidatus* Competibacter (GAOmix). Z-stack images are represented as maximum intensity projections. The channel visualizing the EUBmix probe is included as a reference to distinguish unstained regions from voids and to ensure that the organism of interest is detectable by the FISH protocol.

Candidatus Competibacter occurred in spherical clusters of 9.28 +/− 3.79 μm ($N = 9$) in diameter in the inoculum from industrial origin. Similar morphologies were observed in both reactors throughout Stage 1, after which the fluorescent signal was more spread out in Stages 2 and 3. *Zoogloea* occurred in typical irregular clusters. These morphologies and abundances roughly correspond to the results observed earlier for ThT staining, except for the inoculum from municipal original where a scarce and scattered signal was observed.

Sequential ThT staining and FISH were performed in selected samples with abundant and distinct ThT signals and abundance of the FISH target. Both flash-frozen and 4% PFA fixed samples were used for the initial ThT staining, followed by fixation if needed, and FISH. Both approaches led to similar results. Maximum intensity projections of the sequential results are shown side by side (Fig. 12). As can be observed from the transmission images, dehydration and drying steps included in the FISH procedure led to a shrinking and distortion of the sludge flocs. Taking this into account, *Ca.* Competibacter and *Zoogloea* tested often (but not always) ThT positive. Knowing that the used probes target various subpopulations, this could indicate that only selected strains produce detectable amyloids under the applied conditions.

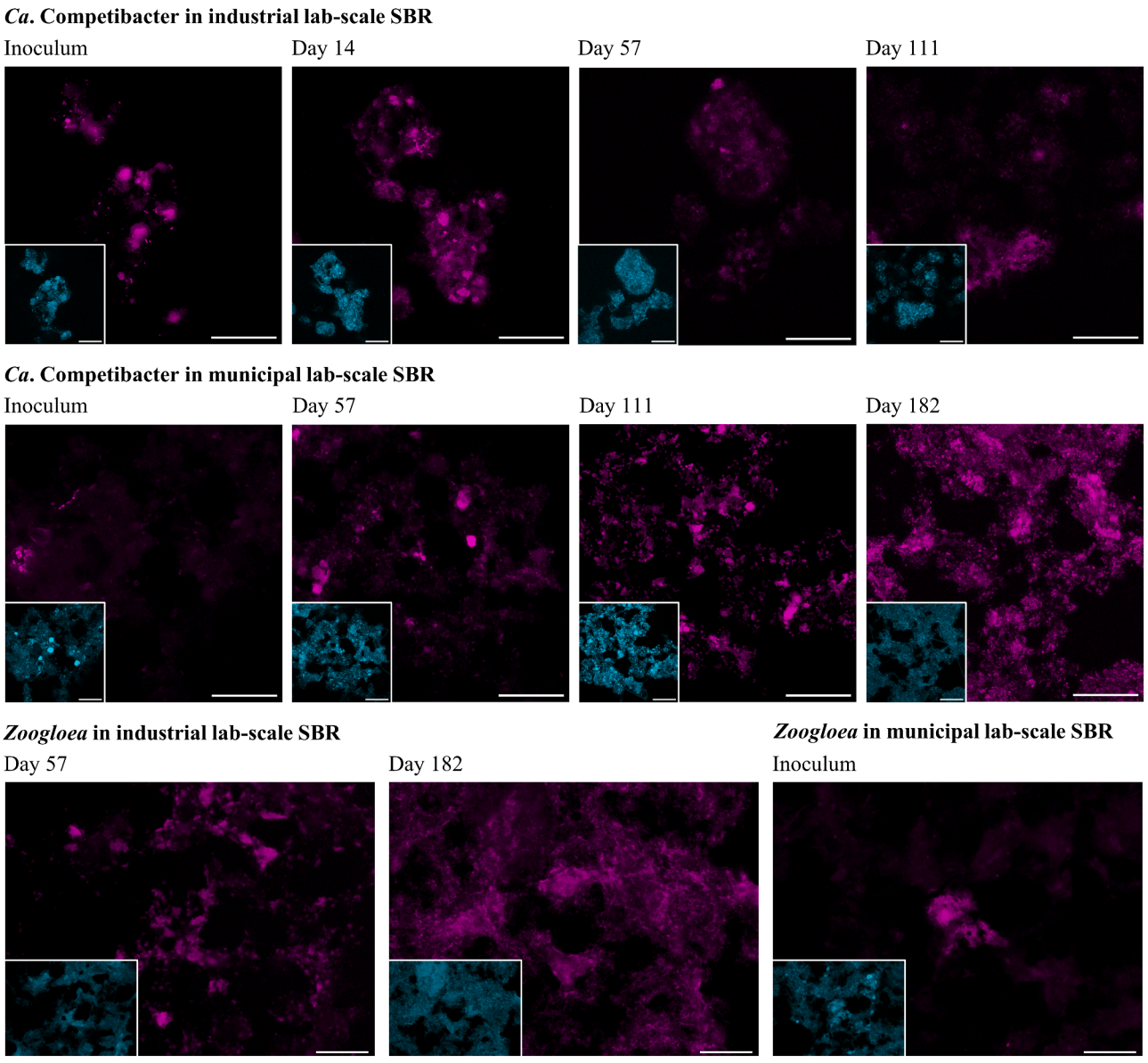

Fig. 11. Representative fluorescence CLSM images illustrating the evolution of spatial distribution of potential amyloid producers in sludge flocs in the sequencing batch reactors (SBRs). Samples stained with oligonucleotide probes targeting *Candidatus* Competibacter (GAOmix) or *Zoogloea* (ZRA23a) (magenta) and Bacteria (EUBmix, cyan). Results shown for inoculum and Stage 1 (day 14 and 57), the end of Stage 2 (day 111) and the end of Stage 3 (day 182) where sludge was subjected to feeding once every 6 h, 72 min, and 20 min, respectively. Z-stacks represented as maximum intensity projections. Scale bar = 50 μm.

4. Discussion

The focus of this study was to investigate whether the feeding pattern could stimulate or repress amyloid production in a targeted way, while considering the compositional evolution of the bacterial community, with a focus on amyloid producers. Additionally, in order to improve our understanding of the function of amyloids, the results of rigorous monitoring of the distribution of the amyloid-positive fraction are discussed, as well as the potential link with bioflocculation performance indicators such as floc size and shear sensitivity.

4.1. Evolution of the Thioflavin T detected amyloids versus the feeding conditions

The ThT fluorescent signal increased quickly both in sludge initially containing a higher amount of amyloids (industrial SBR) and in sludge initially containing a negligible amount of amyloids (municipal SBR), and remained high throughout the experiment. This implies an increased production of amyloid adhesins, an increased abundance of amyloid producers, or both.

Several parameters were potentially beneficial for amyloid production in the reactors, such as the composition of the wastewater, the design of the reactor and the feeding regime. As for the composition of the wastewater, the carbon source calcium acetate introduces Ca^{2+}-ions, which are known to promote amyloid formation in the context of neurodegenerative disorders (Botelho et al., 2012; Itkin et al., 2011). In addition, the mechanical design of the reactor with effluent removal from the top might also have contributed, by selecting for the best settling flocs. This contribution is, however, expected to be minor since no observable biomass was present in the supernatant after the 20 min settling phase. Moreover, later in-house experiments with similar inoculum and operational conditions but with a membrane retrofitted to the SBR setup, also showed a similar rapid increase of ThT fluorescence (results not shown).

The most important and intended impact was the feast-famine feeding regime, which was hypothesized to improve the production of

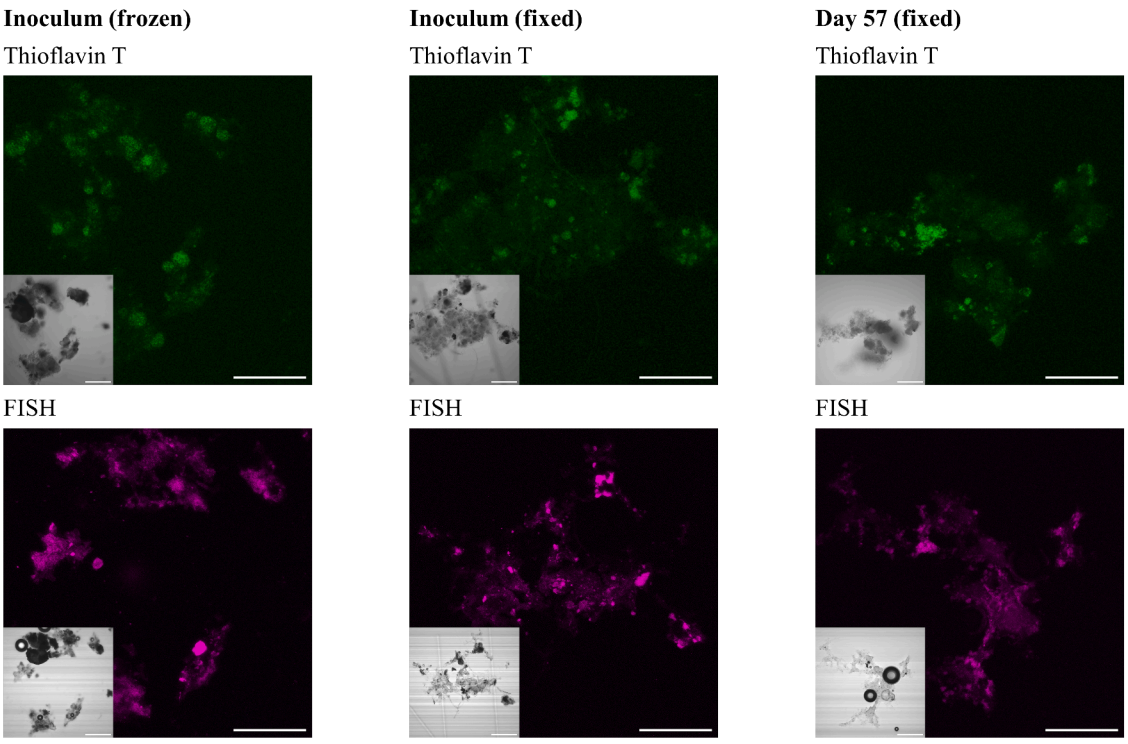

Fig. 12. Fluorescence CLSM and transmission images for the identification of amyloid producers in activated sludge from industrial lab-scale sequencing batch reactor. Sequential staining by 3 μM Thioflavin T (green) and oligonucleotide probes (magenta) targeting several *Ca.* Competibacter (GAOmix, inoculum) and several *Zoogloea* (ZRA23a, day 57). Z-stacks represented as maximum intensity projections. Transmission images included in gray. Circular air bubbles trapped in mounting agent are visible in some transmission images. Scale bar = 50 μm.

amyloids in the sludge. In general, the typical feast-famine SBR operation is known to induce good microbial aggregation which relates to strong binding forces (Gao et al., 2011). More specifically, the positive effect of starvation on amyloid production has indeed been reported before in mixed bacterial communities in the context of drinking water biofilms, and pure culture biofilms (Gerstel and Römling, 2001; Larsen et al., 2007). These feast-famine conditions were created in operational Stage 1 by feeding once every 6 h and later alleviated in operational Stages 2 and 3 by feeding once every 72 and 20 min. Unexpectedly, the ThT fluorescence signal remained high when feast-famine conditions were alleviated. By feeding on a more regular basis, not all organic carbon was consumed during the anoxic phase. Hence, in Stages 2 and 3 part of the feeding was applied during the aerated reaction phase, most likely strongly affecting the microbial community. This will be discussed next.

4.2. Abundance and identity of potential amyloid producers

Sequencing results were screened for potential amyloid producers by focusing on (*i*) highly abundant genera and (*ii*) known EPS and amyloid producers.

In the industrial lab-scale SBR, the abundance of *Zoogloea* coincided with the increase in ThT fluorescence observed during the first 62 days of reactor operation. *Zoogloea* is a well-known EPS producer and "slime former" (An et al., 2016; Characklis, 1973), and its production of amyloids has been confirmed in pure and mixed culture via ThT staining, but not by antibody staining (Larsen et al., 2008). Here, we confirm ThT-stained *Zooglea* in a mixed microbial culture. Note that ThT can bind to cellulose fibers which can be produced by *Zoogloea* and other organisms and are associated with flocculent growth (Retna Raj and Ramaraj, 2001; Friedman et al., 1968; Deinema and Zevenhuizen, 1971). If the ThT staining near *Zoogloea* stems from interactions with cellulose instead of amyloids, then this signal might still imply a role in bioflocculation for *Zoogloea* through its cellulose fibrils. *Zooglea* belongs to the family *Rhodocyclaceae* in which also other EPS-producing denitrifiers are also classified, including *Thauera* (Shinoda et al., 2004; Szabó et al., 2017). *Thauera* is in this experiment mainly detected during the first operational stage in both industrial and municipal lab-scale SBR. *Thauera*'s amyloid-producing properties in activated sludge have been confirmed before via ThT staining (Larsen et al., 2008). During later operational stages the EPS-producing denitrifier *Flavobacterium* of the family *Flavobacteriaceae* was very abundant in the industrial lab-scale reactor as also indicated by Li et al. (2014).

Furthermore, actinobacterial PAOs have been identified as potential amyloid producers via ThT staining (Larsen et al., 2008). The genera *Tetrasphaera* and *Dechloromonas* were detected in the first stage of reactor operation in the municipal lab-scale SBR but their abundance did not coincide with the observed ThT fluorescence in later stages (decreasing or high but gone after the first operational stage, respectively). Given that the synthetic wastewater did not contain much phosphate, it is logical that PAOs were not functionally promoted.

In later operational stages with aerobic feeding, the bacterial community in the industrial lab-scale SBR was mainly dominated by *Zoogloea* and *Flavobacterium*, both fast-growing heterotrophs that can use O_2 or NO_3^- as terminal electron acceptors (Rosenberg et al., 2014). The nitrifiers, on the other hand, were washed out once the feast-famine conditions were alleviated. Most probably, they lost the competition for oxygen against the fast-growing heterotrophs when organic carbon was still available during the aerated phase.

In contrast, fewer *Zoogloea* and *Flavobacterium* were detected in the municipal lab-scale SBR but there the abundance of the glycogen accumulating *Candidatus* Competibacter steadily increased. Genomic analyses indicated the potential for full denitrification in a member from this genus (McIlroy et al., 2014). Similarly, Weissbrodt et al. (2013) noticed that *Zoogloea* were never abundant in the biomass of their GAO-SBR. Nevertheless, populations with a dominance of either *Zoogloea* or *Candidatus* Competibacter both showcased good flocculation performance up to aerobic granules formation. The sequential ThT

staining and FISH procedure in our study seems indeed to imply the possibility of amyloid production by *Candidatus* Competibacter. In contrast, research performed on full-scale WWTP samples reported no binding of antibody or ThT to the GAOmix- or general *Gammaproteobacteria*-probe defined group (Larsen et al., 2008). This might indicate that some micro-organisms only express amyloids under certain conditions. In any case, validation of results via, e.g., staining with antibodies is advised.

In other research fields, glycogen has been reported to accelerate fibril formation in the hen egg-white lysozyme model system (Holubová et al., 2021). In the domain of wastewater treatment, it is known that colonies of *Gammaproteobacteria*, to which *Candidatus* Competibacter are related, are very resistant to shear, implying strong cell-to-cell interactions in the microcolonies (Klausen et al., 2004). This result could be related to the presence of EPS components such as amyloids, also supported by the observation that the removal of Ca^{2+} ions leads to the weakening of these interactions. However, Klausen et al. additionally reported the low dependency on hydrophobic interactions in *Gammaproteobacterial* aggregates, which does not support the above statement. Finally, Dominiak et al. (2011) reported *Candidatus* Competibacter being consistently surrounded by eDNA, inferring that this eDNA might enhance the strength of its microcolonies. It should be noted that DNA is a molecule with a repeating structure with a possibility of unspecific binding by ThT (Ilanchelian and Ramaraj, 2004). Again, checking the current results with other dyes is recommended.

Finally, it was observed that some of the above-mentioned potential amyloid producers were already present in the inoculum from municipal origin when almost no amyloids were detected fluorescently. This was the case for some *Actinobacterial* PAOs (*Dechloromonas* 4.80%, *Tetrasphaera* 3.85%) and *Zoogloea* (3.54%). This lack of amyloid signal might be explained by the absence of the growth conditions triggering the expression of amyloid adhesins in the full-scale WWTP of origin. This again highlights the importance of understanding these conditions.

4.3. Distribution and location of the Thioflavin T-positive fraction

A diversity of ThT positive areas have been observed throughout all stages of this study, potentially indicating the diverse functions of amyloid interactions in activated sludge flocs.

Firstly, ThT fluorescence was observed as distinct clusters indicating the presence of amyloids within microcolonies of certain organisms. This distinct localization occurred mainly in the industrial lab-scale SBR and during the first stage of reactor operation. Larsen et al. similarly observed amyloids mostly in microcolonies using ThT and WO1 and WO2 conformational antibodies, in case of non-filamentous bacteria and in full-scale samples. Amyloids can, hence, potentially improve internal adhesion within microcolonies (Larsen et al., 2008).

Secondly, ThT fluorescence was observed dispersed throughout the bacterial floc. This dispersed appearance occurred mainly in the municipal reactor and during the later stages of reactor operation, potentially as a result of scattering of the amyloid producers throughout the floc, or a wider variety of micro-organisms being able to produce amyloids in the applied cultivation conditions. This disperse presence of adhesins might help bio-aggregation by increasing the hydrophobicity of the overall floc (Larsen et al., 2008). Aqeel et al. (2021) and Brei et al. (2011) also reported this scattered presence of amyloids via immunohistochemical detection with antibodies against CsgA and CsgB curli proteins in sludge samples from lab-scale fixed-film SBR and a full-scale communal WWTP, respectively. It was, however, not possible to confirm their observation that curli amyloids were more abundant near the core of the granule or floc, respectively, since no reference staining, targeting all biomass, was included in these papers.

Thirdly, amyloids were present on filamentous bacteria, which has been observed before by means of ThT or WO1 antibody staining (Conco et al., 2018; Larsen et al., 2008). It is hypothesized that amyloids might also positively affect the floc strength via strengthening the sheaths of these filamentous bacteria that are important as floc backbone (Larsen et al., 2008), but no further research has been performed thus far on the identification of these filamentous amyloid-producing bacteria.

4.4. Effect of abundance, morphology and location of ThT-positive fraction on bioflocculation

In the industrial lab-scale SBR, the presence of amyloids in distinct clusters corresponded to a high average floc size while a disperse morphology corresponded to a lower average floc size. This might be explained by the adhesion mechanisms induced by the amyloid adhesins: when amyloids occur in tightly packed dense clusters, both hydrophobic interactions as well as physical entanglement can take place and contribute to the total adhesion strength. This provides tightly bound building blocks. On the contrary, when amyloids occur more disperse, physical protein-to-protein interactions are less prominent, and the adhesion strength is mainly a result of the hydrophobic interactions. These changing interactions are not reflected, however, in the floc shear sensitivity data. Note that even in our adjusted protocol, the shear sensitivity measurement is still prone to a large variability and that it reflects the amount of sheared off primary particles and does not give information about the strength of the sludge floc as a whole. Additionally, the potential impact of other EPS components and corresponding interactions, whose evolution has not been monitored throughout the experiment, should be acknowledged.

4.5. Comments on the applied procedures

Relative quantification of Thioflavin T fluorescence. Quantification of the ThT signal is typically performed in monoprotein experiments, i.e., to monitor fibrillation of protein solutions (LeVine, 1999; Morel et al., 2010) or decay of amyloids fibrils (Morales-Belpaire and Gerin, 2008), and rarely in biofilms of pure cultures of micro-organisms (Randrianjatovo-Gbalou et al., 2017). The intensity of bound ThT is known to vary with (*i*) environmental conditions (e.g., temperature, solvent), (*ii*) the total applied ThT concentration, and (*iii*) the nature and concentration of proteins (Amdursky et al., 2012; Xue et al., 2017). The proposed protocol avoids some of these variations, e.g., by fixing the applied ThT concentration at 3 μM and the biomass content at 1 g MLSS L^{-1}. Still, the amyloid protein-dependent ThT intensity will always inherently affect the signal since activated sludge is a mixed and evolving community of bacteria. Therefore, the reported quantity of ThT fluorescence should not be directly linked to amyloid concentration. Rather, it gives an impression of trends in the amyloid production.

Unspecific binding of Thioflavin T. When detecting amyloids using the conformational dye Thioflavin T in complex biological samples, one should be aware that unspecific binding to interfering components such as cellulose, mentioned before in the context of *Zoogloea*, and extracellular DNA might contribute to the signal (Ilanchelian and Ramaraj, 2004; Retna Raj and Ramaraj, 2001). It should be noted that the authors did not observe the latter interference (verified by experiments combining the cell-impermeable nucleic acid stain propidium iodide and Thioflavin T). A thorough microscopic investigation at several timepoints (e.g., detecting cellulose fibers in municipal inoculum) might help to critically assess qualitative and quantitative results.

Sequential detection method. When using ThT to stain amyloids, the sequential method is needed since the ThT signal cannot be detected after FISH. This might be due to formic acid denaturation of proteins during the hybridization step (Christensen et al., 2020). Fresh samples lead to the highest observable ThT signal but both fixed and flash-frozen samples have been used successfully in this work. For those cases, the ThT signal was much weaker, potentially due to partial crosslinking of the targets, or damage from ice crystals (although amyloids are stable upon freezing: e.g., Schoonenboom et al. (2005) reported no lower relative concentration of amyloid β (1–42) protein after one freeze/thaw

cycle).

4.6. Future research

Identification of amyloid producers in mixed culture via FISH, first applied by Larsen et al. (2007), is a powerful method as most bacteria in environmental samples remain uncultured (Larsen et al., 2008). However, the method is partly based on trial-and-error, investigating a few potential amyloid producers at a time. To have complementary information, ongoing research focuses on proteome characterization such as also performed by Silva et al. (2012). Successful implementation of this method requires a complete extraction of the tightly bound EPS and overcoming interferences by other matrix components.

To screen the conditions that trigger amyloid production, relevant amyloid-producing wastewater treatment-related organisms could be studied in controllable aggregation formats such as biofilms. This approach has been implemented before with *Salmonella, Pseudomonas*, and *Escherichia* model organisms (Gerstel and Römling, 2001; Maurer et al., 1998; Prigent-Combaret et al., 2001; Scharfman et al., 1996). Conclusions from this biofilm format could help to understand observations in flocs or granules since biological aggregation can be considered a continuum (Aqeel et al., 2019). To still mimic the complex interactions and dynamics within mixed communities, co-cultures that encompass several functional strains (e.g., nitrifiers and denitrifiers) can be envisaged.

5. Conclusion

In this experimental study, the effect of various feeding regimes on amyloids and potential amyloid producers in activated sludge was rigorously monitored over 183 days. To this end, the fluorescent dye Thioflavin T was used qualitatively and quantitatively. The abundance of detectable amyloids was enhanced in SBRs fed with synthetic wastewater, and this in sludges containing a negligible or already substantial amount of amyloids upon inoculation. The feeding regime impacted the distribution of produced amyloids: feast-famine conditions resulted in dense clusters while nearly continuous feeding resulted in dispersion of the detected amyloids. The initial hypothesis that a more continuous feeding phase would negatively impact the sludge bioflocculation was not confirmed. While the average floc size did decrease towards the nearly continuous feeding phase for the industrial SBR, the floc size remained the same for the municipal sludge throughout the experiment with also no clear impact on the shear sensitivity of the sludges. However, the feeding regime clearly impacted the bacterial community: more continuous and, thereby partly aerobic feeding resulted in a dominance of denitrifiers, owing to their ability to exploit oxygen as electron acceptor when there is still organic carbon present. This included the potential amyloid producer *Zoogloea* in the industrial lab-scale reactor. Furthermore, the glycogen accumulating *Candidatus* Competibacter were or became dominant in both reactors. This research is the first to identify *Candidatus* Competibacter as a potential amyloid producer based on sequential Thioflavin T staining and FISH. These results highlight the importance of the interplay between the presence of growth conditions triggering amyloid production and varying bacterial communities in which amyloid producers can become dominant.

Declaration of Competing Interest

The authors declare that they have no known competing financial interests or personal relationships that could have appeared to influence the work reported in this paper.

The authors declare no competing interests.

Data availability

Data will be made available on request.

Acknowledgments

An-Sofie Christiaens holds a Ph.D. grant for Strategic Basic Research from the Research Foundation-Flanders (FWO-1S41420N). Aquafin and Pantarein Water (Belgium) are acknowledged for providing sludge samples. We thank Johan Martens and Tom Bosserez (KU Leuven) for providing access to the Tecan Infinite M200 Pro microplate reader, and Johan Hofkens and Rik Nuyts (KU Leuven) for providing access to the Olympus confocal FluoView™ FV1000 microscope.

References

Amann, R., 1995. *In situ* identification of micro-organisms by whole cell hybridization with rRNA-targeted nucleic acid probes. in: Mol. Microb. Ecol. Man. https://doi.org/10.1007/978-94-011-0351-0_23.

Amann, R.I., Binder, B.J., Olson, R.J., Chisholm, S.W., Devereux, R., Stahl, D.A., 1990. Combination of 16S rRNA-targeted oligonucleotide probes with flow cytometry for analyzing mixed microbial populations. Appl. Environ. Microbiol. 56, 1919–1925. https://doi.org/10.1128/aem.56.6.1919-1925.1990.

Amdursky, N., Erez, Y., Huppert, D., 2012. Molecular rotors: what lies behind the high sensitivity of the thioflavin-T fluorescent marker. Acc. Chem. Res. 45, 1548–1557. https://doi.org/10.1021/ar300053p.

An, W., Guo, F., Song, Y., Gao, N., Bai, S., Dai, J., Wei, H., Zhang, L., Yu, D., Xia, M., Yu, Y., Qi, M., Tian, C., Chen, H., Wu, Z., Zhang, T., Qiu, D., 2016. Comparative genomics analyses on EPS biosynthesis genes required for floc formation of *Zoogloea resiniphila* and other activated sludge bacteria. Water Res. 102, 494–504. https://doi.org/10.1016/j.watres.2016.06.058.

Aqeel, H., Basuvaraj, M., Liss, S.N., 2021. Microbial population selection in integrated fixed-film sequencing batch reactors operated with different lengths of oxic and anoxic conditions. Environ. Sci. Water Res. Technol. 7, 913–926. https://doi.org/10.1039/d0ew01022g.

Aqeel, H., Weissbrodt, D.G., Cerruti, M., Wolfaardt, G.M., Wilén, B.M., Liss, S.N., 2019. Drivers of bioaggregation from flocs to biofilms and granular sludge. Environ. Sci. Water Res. Technol. 5, 2072–2089. https://doi.org/10.1039/c9ew00450e.

Biancalana, M., Koide, S., 2010. Molecular mechanism of thioflavin-T binding to amyloid fibrils. Biochim. Biophys. Acta 1804, 1405–1412. https://doi.org/10.1016/j.bbapap.2010.04.001.Molecular.

Bolyen, E., Rideout, J.R., Dillon, M.R., et al., 2019. Reproducible, interactive, scalable and extensible microbiome data science using QIIME 2. Nat. Biotechnol. 37, 852–857. https://doi.org/10.1038/s41587-019-0209-9.

Botelho, H.M., Leal, S.S., Cardoso, I., Yanamandra, K., Morozova-Roche, L.A., Fritz, G., Gomes, C.M., 2012. S100A6 amyloid fibril formation is calcium-modulated and enhances superoxide dismutase-1 (SOD1) aggregation. J. Biol. Chem. 287, 42233–42242. https://doi.org/10.1074/jbc.M112.396416.

Brei, E., 2011. Bacterial Adhesin Proteins Associated with Microbial Flocs and EPS in the Activated Sludge. University of Toronto.

Chapman, M.R., Robinson, L.S., Pinkner, J.S., Roth, R., Heuser, J., Hammar, M., Normark, S., Hultgren, S.J., 2002. Role of *Escherichia coli* Curli Operons in directing amyloid fiber formation. Science 295 (80–), 851–855. https://doi.org/10.1126/science.1067484.Role.

Characklis, W.G., 1973. Attached microbial growths. Water Res. 7, 1113–1127. https://doi.org/10.1016/0043-1354(73)90066-3.

Christensen, L.F.B., Nowak, J.S., Sønderby, T.V., Frank, S.A., Otzen, D.E., 2020. Quantitating denaturation by formic acid: imperfect repeats are essential to the stability of the functional amyloid protein FapC. J. Biol. Chem. 295, 13031–13046. https://doi.org/10.1074/jbc.ra120.013396.

Conco, T., Kumari, S., Stenström, T., Bux, F., 2018. Epibiont growth on filamentous bacteria found in activated sludge: a morphological approach. Arch. Microbiol. 200, 493–503. https://doi.org/10.1007/s00203-017-1461-3.

Crocetti, G.R., Banfield, J.F., Keller, J., Bond, P.L., Blackall, L.L., 2002. Glycogen-accumulating organisms in laboratory-scale and full-scale wastewater treatment processes. Microbiology 148, 3353–3364. https://doi.org/10.1099/00221287-148-11-3353.

Daims, H., Brühl, A., Amann, R., Schleifer, K.H., Wagner, M., 1999. The domain-specific probe EUB338 is insufficient for the detection of all *Bacteria*: development and evaluation of a more comprehensive probe set. Syst. Appl. Microbiol. 22, 434–444. https://doi.org/10.1016/S0723-2020(99)80053-8.

De Ferrari, G.V., Mallender, W.D., Inestrosa, N.C., Rosenberry, T.L., 2001. Thioflavin T is a fluorescent probe of the acetylcholinesterase peripheral site that reveals conformational interactions between the peripheral and acylation sites. J. Biol. Chem. 276, 23282–23287. https://doi.org/10.1074/jbc.M009596200.

Deinema, M.H., Zevenhuizen, L.P.T.M., 1971. Formation of cellulose fibrils by gram-negative bacteria and their role in bacterial flocculation. Arch. Mikrobiol. 78, 42–57. https://doi.org/10.1007/BF00409087.

Dominiak, D.M., Nielsen, J.L., Nielsen, P.H., 2011. Extracellular DNA is abundant and important for microcolony strength in mixed microbial biofilms. Environ. Microbiol. 13, 710–721. https://doi.org/10.1111/j.1462-2920.2010.02375.x.

Dueholm, M.S., Nielsen, P.H., Flemming, H.C., Neu, T.R., Wingender, J., 2016. Amyloids – a neglected child of the slime. The Perfect Slime : Microbial Extracellular Polymeric Substances (EPS), Eds. IWA Publishing, London, pp. 113–133. https://doi.org/10.2166/9781780407425.

Epstein, E.A., Chapman, M.R., 2008. Polymerizing the fibre between bacteria and host cells: the biogenesis of functional amyloid fibres. Cell. Microbiol. 10, 1413–1420. https://doi.org/10.1111/j.1462-5822.2008.01148.x.

Friedman, B.A., Dugan, P.R., Pfister, R.M., Remsen, C.C., 1968. Fine structure and composition of the zoogloeal matrix surrounding *Zoogloea ramigera*. J. Bacteriol. 96, 2144–2153. https://doi.org/10.1128/jb.96.6.2144-2153.1968.

Gao, D., Liu, L., liang, H., Wu, W.M., 2011. Comparison of four enhancement strategies for aerobic granulation in sequencing batch reactors. J. Hazard. Mater. 186, 320–327. https://doi.org/10.1016/j.jhazmat.2010.11.006.

Gerstel, U., Römling, U., 2001. Oxygen tension and nutrient starvation are major signals that regulate *agfD* promoter activity and expression of the multicellular morphotype in *Salmonella typhimurium*. Environ. Microbiol. 3, 638–648. https://doi.org/10.1046/j.1462-2920.2001.00235.x.

Greenberg, A., Clesceri, L.S., Eaton, A.D, 1992. Standard Methods for the Examination of Water and Wastewater, 18th ed. American Public Health Association (APHA) Publications. https://doi.org/10.2105/AJPH.51.6.940-a.

Holubová, M., Lobaz, V., Loukotová, L., Rabyk, M., Hromádková, J., Trhlíková, O., Pechrová, Z., Groborz, O., Štěpánek, P., Hrubý, M., 2021. Does polysaccharide glycogen behave as a promoter of amyloid fibril formation at physiologically relevant concentrations? Soft Matter 17, 1628–1641. https://doi.org/10.1039/d0sm01884h.

Ilanchelian, M., Ramaraj, R., 2004. Emission of thioflavin T and its control in the presence of DNA. J. Photochem. Photobiol. A Chem. 162, 129–137. https://doi.org/10.1016/S1010-6030(03)00320-4.

Itkin, A., Dupres, V., Dufrêne, Y.F., Bechinger, B., Ruysschaert, J.M., Raussens, V., 2011. Calcium ions promote formation of amyloid β-peptide (1-40) oligomers causally implicated in neuronal toxicity of Alzheimer's disease. PLoS One 6. https://doi.org/10.1371/journal.pone.0018250.

Jenné, R., Banadda, E.N., Smets, I., Deurinck, J., Van Impe, J., 2007. Detection of filamentous bulking problems: developing an image analysis system for sludge composition monitoring. Microsc. Microanal. 13, 36–41. https://doi.org/10.1017/S1431927607070092.

Klausen, M.M., Thomsen, T.R., Nielsen, J.L., Mikkelsen, L.H., Nielsen, P.H., 2004. Variations in microcolony strength of probe-defined bacteria in activated sludge flocs. FEMS Microbiol. Ecol. 50, 123–132. https://doi.org/10.1016/j.femsec.2004.06.005.

Klindworth, A., Pruesse, E., Schweer, T., Peplies, J., Quast, C., Horn, M., Glöckner, F.O., 2013. Evaluation of general 16S ribosomal RNA gene PCR primers for classical and next-generation sequencing-based diversity studies. Nucleic Acids Res. 41, 1–11. https://doi.org/10.1093/nar/gks808.

Kong, Y., Ong, S.L., Ng, W.J., Liu, W.T., 2002. Diversity and distribution of a deeply branched novel proteobacterial group found in anaerobic-aerobic activated sludge processes. Environ. Microbiol. 4, 753–757. https://doi.org/10.1046/j.1462-2920.2002.00357.x.

Larsen, P., Nielsen, J.L., Dueholm, M.S., Wetzel, R., Otzen, D., Nielsen, P.H., 2007. Amyloid adhesins are abundant in natural biofilms. Environ. Microbiol. https://doi.org/10.1111/j.1462-2920.2007.01418.x.

Larsen, P., Nielsen, J.L., Otzen, D., Nielsen, P.H., 2008. Amyloid-like adhesins produced by floc-forming and filamentous bacteria in activated sludge. Appl. Environ. Microbiol. https://doi.org/10.1128/AEM.02274-07.

Lemoine, L., Verbeke, M., Bernaerts, K., Springael, D., 2019. Impact of the inoculum composition on the structure of the total and active community and its performance in identically operated anaerobic reactors. Appl. Microbiol. Biotechnol. 103, 9191–9203. https://doi.org/10.1007/s00253-019-10041-8.

LeVine, H., 1999. Quantification of β-sheet amyloid fibril structures with thioflavin T. Methods Enzymol. 309, 274–284. https://doi.org/10.1016/S0076-6879(99)09020-5.

Li, J., Ding, L.B, Cai, A., Huang, G.X., Horn, H., 2014. Aerobic sludge granulation in a full-scale sequencing batch reactor. Biomed. Res. Int. https://doi.org/10.1155/2014/268789.

Lin, Y., Reino, C., Carrera, J., Pérez, J., van Loosdrecht, M.C.M., 2018. Glycosylated amyloid-like proteins in the structural extracellular polymers of aerobic granular sludge enriched with ammonium-oxidizing bacteria. Microbiologyopen 7, 1–13. https://doi.org/10.1002/mbo3.616.

Loy, A., Maixner, F., Wagner, M., Horn, M., 2007. probeBase - an online resource for rRNA-targeted oligonucleotide probes: new features 2007. Nucleic Acids Res. 35, 800–804. https://doi.org/10.1093/nar/gkl856.

Maurer, J.J., Brown, T.P., Steffens, W.L., Thayer, S.G., 1998. The occurrence of ambient temperature-regulated adhesins, curli, and the temperature-sensitive hemagglutinin Tsh among avian *Escherichia coli*. Avian Dis. 42, 106–118. https://doi.org/10.2307/1592582.

McIlroy, S.J., Albertsen, M., Andresen, E.K., Saunders, A.M., Kristiansen, R., Stokholm-Bjerregaard, M., Nielsen, K.L., Nielsen, P.H., 2014. `*Candidatus* Competibacter'-lineage genomes retrieved from metagenomes reveal functional metabolic diversity. ISME J. 8, 613–624. https://doi.org/10.1038/ismej.2013.162.

Mikkelsen, L.H., Keiding, K., 2002. The shear sensitivity of activated sludge: an evaluation of the possibility for a standardised floc strength test. Water Res. https://doi.org/10.1016/S0043-1354(01)00518-8.

Morales-Belpaire, I., Gerin, P.A., 2008. Fate of amyloid fibrils introduced in wastewater sludge. Water Res. 42, 4449–4456. https://doi.org/10.1016/j.watres.2008.07.034.

Morel, B., Varela, L., Azuaga, A.I., Conejero-Lara, F., 2010. Environmental conditions affect the kinetics of nucleation of amyloid fibrils and determine their morphology. Biophys. J. 99, 3801–3810. https://doi.org/10.1016/j.bpj.2010.10.039.

Nielsen, P.H., Daims, H., Lemmer, H., 2009. FISH Handbook for Biological Wastewater Treatment: Identification and Quantification of Microorganisms in Activated Sludge and Biofilms by FISH. IWA Publishing, London.

O'Nuallain, B., Wetzel, R., 2002. Conformational Abs recognizing a generic amyloid fibril epitope. Proc. Natl. Acad. Sci. U. S. A. 99, 1485–1490. https://doi.org/10.1073/pnas.022662599.

Prigent-Combaret, C., Brombacher, E., Vidal, O., Ambert, A., Lejeune, P., Landini, P., Dorel, C., 2001. Complex regulatory network controls initial adhesion and biofilm formation in *Escherichia coli* via regulation of the *csgD* gene. J. Bacteriol. 183, 7213–7223. https://doi.org/10.1128/JB.183.24.7213-7223.2001.

Quast, C., Pruesse, E., Yilmaz, P., Gerken, J., Schweer, T., Yarza, P., Peplies, J., Glöckner, F.O., 2013. The SILVA ribosomal RNA gene database project: improved data processing and web-based tools. Nucleic Acids Res. 41, 590–596. https://doi.org/10.1093/nar/gks1219.

Randrianjatovo-Gbalou, I., Rouquette, P., Lefebvre, D., Girbal-Neuhauser, E., Marcato-Romain, C.E., 2017. *In situ* analysis of *Bacillus licheniformis* biofilms: amyloid-like polymers and eDNA are involved in the adherence and aggregation of the extracellular matrix. J. Appl. Microbiol. 122, 1262–1274. https://doi.org/10.1111/jam.13423.

Retna Raj, C., Ramaraj, R., 2001. Emission of Thioflavin T and its off–on control in polymer membranes. J. Photochem. Photobiol. A Chem. 74, 129–137. https://doi.org/10.1016/S1010-6030(03)00320-4.

Rosenberg, E., DeLong, E.F., Lory, S., Stackebrandt, E., Thompson, F., 2014. The Prokaryotes, 4th ed. Springer Berlin, Heidelberg. https://doi.org/10.1007/978-3-642-30197-1.

Rosselló-Mora, R.A., Wagner, M., Amann, R., Schleifer, K.H., 1995. The abundance of *Zoogloea ramigera* in sewage treatment plants. Appl. Environ. Microbiol. 61, 702–707. https://doi.org/10.1128/aem.61.2.702-707.1995.

Scharfman, A., Kroczynski, H., Carnoy, C., Van Brussel, E., Lamblin, G., Ramphal, R., Roussel, P., 1996. Adhesion of *Pseudomonas aeruginosa* to respiratory mucins and expression of mucin-binding proteins are increased by limiting iron during growth. Infect. Immun. 64, 5417–5420. https://doi.org/10.1128/iai.64.12.5417-5420.1996.

Schindelin, J., Arganda-Carreras, I., Frise, E., Kaynig, V., Longair, M., Pietzsch, T., Cardona, A., 2012. Fiji: an open-source platform for biological-image analysis. Nat. Methods 9, 676–682. https://doi.org/10.1038/nmeth.2019.

Schoonenboom, N.S.M., Mulder, C., Vanderstichele, H., Van Elk, E.J., Kok, A., Van Kamp, G.J., Scheltens, P., Blankenstein, M.A., 2005. Effects of processing and storage conditions on amyloid β (1-42) and tau concentrations in cerebrospinal fluid: implications for use in clinical practice. Clin. Chem. 51, 189–195. https://doi.org/10.1373/clinchem.2004.039735.

Shinoda, Y., Sakai, Y., Uenishi, H., Uchihashi, Y., Hiraishi, A., Yukawa, H., Yurimoto, H., Kato, N., 2004. Aerobic and anaerobic toluene degradation by a newly isolated denitrifying bacterium, thauera sp. strain DNT-1. Appl. Environ. Microbiol. 70, 1385–1392. https://doi.org/10.1128/AEM.70.3.1385-1392.2004.

Silva, A.F., Carvalho, G., Soares, R., Coelho, A.V., Crespo, M.T.B., 2012. Step-by-step strategy for protein enrichment and proteome characterisation of extracellular polymeric substances in wastewater treatment systems. Appl. Microbiol. Biotechnol. 95, 767–776. https://doi.org/10.1007/s00253-012-4157-2.

Suresh, A., Grygolowicz-Pawlak, E., Pathak, S., Poh, L.S., Majid, A., bin, M., Dominiak, D., Bugge, T.V., Gao, X., Ng, W.J., 2018. Understanding and optimization of the flocculation process in biological wastewater treatment processes: a review. Chemosphere 210, 401–416. https://doi.org/10.1016/j.chemosphere.2018.07.021.

Szabó, E., Liébana, R., Hermansson, M., Modin, O., Persson, F., Wilén, B.M., 2017. Microbial population dynamics and ecosystem functions of anoxic/aerobic granular sludge in sequencing batch reactors operated at different organic loading rates. Front. Microbiol. 8, 1–14. https://doi.org/10.3389/fmicb.2017.00770.

Van den Broeck, R., Van Dierdonck, J., Caerts, B., Bisson, I., Kregersman, B., Nijskens, P., Dotremont, C., Van Impe, J., Smets, I., 2010. The impact of deflocculation-reflocculation on fouling in membrane bioreactors. Sep. Purif. Technol. 71, 279–284. https://doi.org/10.1016/j.seppur.2009.12.006.

Weissbrodt, D.G., Neu, T.R., Kuhlicke, U., Rappaz, Y., Holliger, C., 2013. Assessment of bacterial and structural dynamics in aerobic granular biofilms. Front. Microbiol. 4, 1–18. https://doi.org/10.3389/fmicb.2013.00175.

Xue, C., Lin, T.Y., Chang, D., Guo, Z., 2017. Thioflavin T as an amyloid dye: fibril quantification, optimal concentration and effect on aggregation. R. Soc. Open Sci. 4 https://doi.org/10.1098/rsos.160696.